JOURNAL OF AIRCRAFT
Vol. 31, No. 4, July–Aug. 1994

Use of Artificial Neural Networks for Buffet Environments

J. H. Jacobs,* C. E. Hedgecock,† P. F. Lichtenwalner,‡ and L. E. Pado§
McDonnell Douglas Aerospace, St. Louis, Missouri 63166
and
A. E. Washburn¶
ViGYAN Inc., Hampton, Virginia 23666

An artificial neural network-based procedure for predicting empennage buffeting pressures and elastic response as a function of upstream flowfield and geometric conditions has been developed under a cooperative experimental and analytical research agreement between McDonnell Douglas Aerospace (MDA) and NASA Langley Research Center. This research program is a continuing MDA effort to develop a unified buffet design methodology. The current effort employs a hybrid cascading neural network and finite element modeling method to predict flexible tail response based on rigid test pressure information. This method is dependent on experimental data to train the neural network algorithms, but is robust enough to expand its knowledge base with additional aircraft data. Initial results show an incredible potential to predict accurate rms and frequency-dependent tail pressures, as well as flexible response while providing the future capability to incorporate upstream computational fluid dynamics data for advanced design aircraft buffet pressure predictions.

Nomenclature

AOA, α	=	angle of attack
b	=	width of root of flexible tail
$F(n)$	=	contribution to power spectrum of p^2/q^2 in frequency band n
f	=	frequency, Hz
M_{RB}	=	root bending moment
$\mathcal{M}_{RB}$	=	nondimensional root bending moment M_{RB}/qbS
n	=	nondimensional frequency parameter $f \times X/U$
p	=	surface pressure
q	=	freestream dynamic pressure
S	=	surface area of flexible tail
U	=	freestream velocity
X	=	distance from wing apex to Kulite
$\bar{}$	=	rms value

Introduction

FIGHTER aircraft experience high levels of random buffeting pressures on empennage surfaces caused by vortex impingement during critical high AOA maneuvers. These severe random pressure environments can cause shortened structural fatigue lives and premature structural failure. The ability to accurately predict random pressure environments on a vertical tail of a fighter aircraft in the advanced design stage has been quite difficult due to the complexity of the interaction between the aircraft geometry, flowfield, vortex trajectory, and empennage structure. While present aircraft test data can provide an estimate of these dynamic load environments, more accurate and robust prediction methods must be addressed to avoid costly postproduction repairs.

Experimental Research Program

A cooperative research agreement between McDonnell Douglas Aerospace (MDA) and NASA Langley Research Center (NASA LaRC) was established to study the phenomena of vortex tail interactions. Experimental tests have been conducted in the NASA LaRC Basic Aerodynamics Research Tunnel (BART) using the flowfield generated by a 76-deg delta wing with twin vertical tails placed aft of the wing as shown in Fig. 1. This geometrically simple configuration was chosen for this initial study because it contained the pertinent physics involved in the vortex-tail interaction process and reduced undesired aircraft geometric influences. The experimental results are also being used by NASA LaRC to validate computational fluid dynamics (CFD) modeling methods and by MDA to establish an artificial intelligence data base.

The twin-tailed model consisted of the delta wing with the vertical tails mounted on tail support booms aft of the wing. During the investigation, two instrumented tails were used: 1) a rigid tail and 2) a flexible tail. The flexible tail consisted of a single aluminum spar, balsa wood covering, and ballast weights to simulate typical vertical tail responses. The rigid tail was constructed of aluminum and instrumented with five Kulite pressure transducers on each side (Fig. 2). Each tail had nine possible locations relative to the wing, ranging from inboard-forward to outboard-aft. For this investigation only inboard-center and outboard-center were evaluated. The sur-

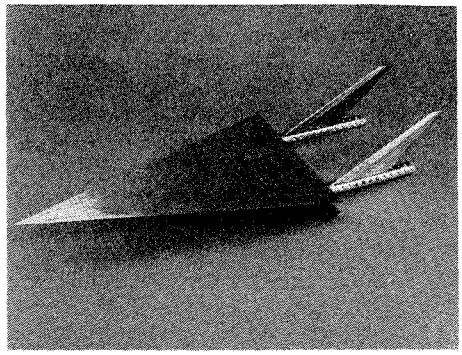

Fig. 1 NASA/MDA wing-vertical tail test model.

Received Feb. 8, 1993; revision received May 19, 1993; accepted for publication July 29, 1993.

*Senior Project Engineer, Structural Dynamics, McDonnell Douglas Corporation. Member AIAA.
†Senior Engineer, Structural Dynamics, McDonnell Douglas Corporation. Member AIAA.
‡Principal Specialist Information Technology, McDonnell Douglas Corporation.
§Senior Specialist Technical Analyst, McDonnell Douglas Corporation.
¶Research Engineer, McDonnell Douglas Corporation. Member AIAA.

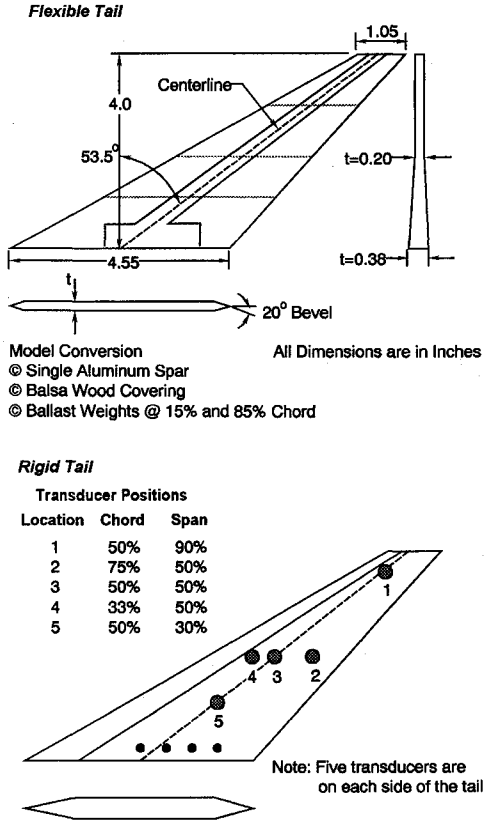

Fig. 2 Rigid and flexible tail configurations.

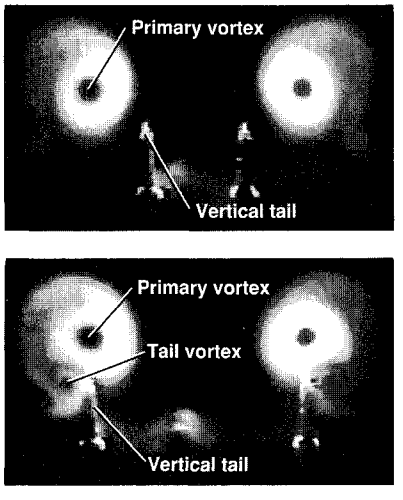

Fig. 3 Tail position effect on vortex flow characteristics (α = 20 deg) (front view).

face pressure fluctuations were used to calculate rms values and power spectral densities (PSD) of the buffet pressures. The buffet pressure is defined as the instantaneous differential pressure between the inboard and the outboard tail transducers.

The experimental investigation has been divided into two distinct phases. The first phase has been completed and its purpose was to examine both the rms magnitude and frequency of the pressures, bending moment, and torsion moment of the tails as functions of flow conditions and AOA. During the second phase of the investigation, the flowfield velocities within the vortices will be measured using a three-component laser Doppler velocimeter (LDV). The velocity data obtained will be used to further expand and refine the vortex-tail interaction models.

The flowfield characteristics of the first phase of the investigation have been documented in a previous publication.[1] Off-body flow visualization was used to examine the vortex structures and the core trajectories for different tail positions as shown in Fig. 3.

When the tails are in the outboard location, the flow visualizations clearly show the presence of a vortex being formed along the leading edge of the tail on the outer surface. The tail vortex was formed due to the combination of the high sweep angle of the vertical tails and the outward spanwise flow from the wing vortex impinging on the tail at an effective AOA. The wing and tail vortices began to interact near the tail tip, and spiraled around one another as they traveled downstream. The tail vortex was stable at all AOA when the tails were at the outboard locations. The relative placement of the tail with the wing vortex location may have eliminated the tail leading-edge vortex for the inboard tail case. The placement of the vertical tail resulted in a reduced sidewash angle in the flow impinging on the tail when compared to the outboard tail location. The flow visualizations indicate that the primary vortex structure using the inboard tails was very similar to the primary vortex structure above the model without tails. The flow visualizations were also used to determine the position of vortex breakdown. The breakdown location was defined by the sudden expansion of the vortex core region that has been attributed to the highly turbulent flow resulting from the breakdown of the vortices upstream of the vertical tails at high AOA.[2,3]

Figure 4 presents the rms buffet pressures near the tip of the rigid tail and the rms bending moments of the flexible tail for both the inboard and the outboard tail positions. The rms buffet pressure and the rms bending moment exhibited similar trends as the angle of attack was increased. Near 30-deg AOA there was a significant increase in the buffeting levels for both

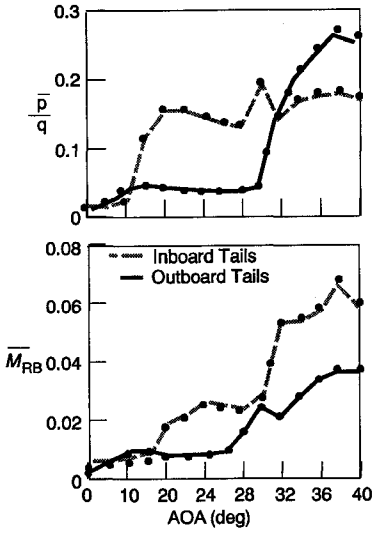

Fig. 4 Typical rigid and flexible rms responses of vertical tails.

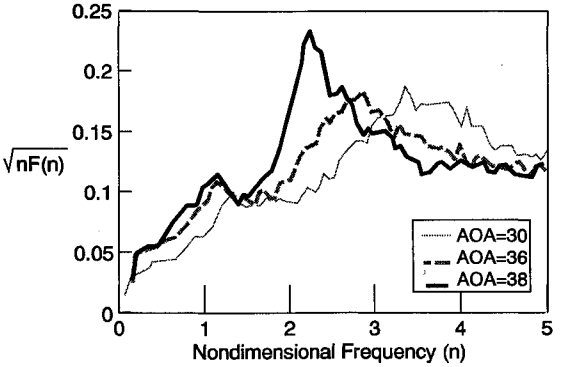

Fig. 5 Nondimensional frequency response of rigid tails for various AOA.

tail positions. This large increase in buffeting corresponds to the movement of the vortex breakdown location upstream of the vertical tails. In addition, as breakdown moves further ahead of the tails, increases and shifting of the PSD peaks was observed. When the breakdown location was upstream of the tails two distinct frequency peaks were observed in the spectra as shown in Fig. 5. These peaks represent coherent fluctuations in the flow. The nondimensional frequency and pressure values presented are characterized using Mabey's[4] method.

It has been shown that frequency spectra measured at chordwise locations can be effectively normalized with local length scale.[5] In following tests, the distance from the vortex breakdown point to the transducer will be used for a more accurate variable length scale. Figure 5 indicates that the frequency content of the vortex downstream of breakdown was also a function of AOA. This will especially affect the flexible tail response if the frequency peak tunes to a natural mode of the elastic structure.

The first phase of the NASA/MDA vortex-tail interaction program has successfully supplied the data base of information necessary for implementation into a buffet neural network system. The same technique will be developed to use upstream velocity contours as input to the neural network. The neural network will be trained with measured velocities. Then, CFD predictions of the flowfield can be used in conjunction with the trained neural network to predict buffeting characteristics of present and future aircraft designs.

Neural Network Modeling

Buffet data are extremely difficult to model using traditional regression techniques due to the multiple number of noisy parameters that interact in a nonlinear manner.[3] Neural networks are especially adept at modeling this kind of data because their interconnected algorithms can accommodate these nonlinearities. They can generally be defined as massively connected, massively parallel networks with the ability to learn. One of their most important characteristics is the ability to generalize from the data they have already seen, which makes them a good candidate for the sparse buffet data. A good source of information on a wide variety of neural network taxonomies is given in Ref. 6.

Root-Mean-Square Data Modeling

It was desired to create a model that could predict the rms pressure $\bar{p}$ at various locations along the rigid tail. Data measurements were provided that gave the pressure as a function of freestream dynamic pressure, angle of attack, tail chord and span of the Kulite sensor positions, and positions of the rigid tail itself in relation to the delta wing. In total, three dynamic pressures ranging from 3.3 to 7.7 psf, 15 AOA ranging from 0 to 40 deg, five Kulite sensor positions, and two tail positions (inboard and outboard) were provided as 450 input/output pairs.

Since these type of buffet pressures are typically not dependent on Mach number,[2,3] it was determined that the dimensionless quantity $\bar{p}/q$ could be used more efficiently than $\bar{p}$ alone, and that the pressure could be recovered later by multiplying by the appropriate dynamic pressure. This left five input parameters with which to predict the pressure ratio $\bar{p}/q$: the AOA, the chord and span location of the sensor, and the fuselage and butt line station of the tail with respect to the delta wing (Fig. 6).

After determining the form of the input and output vectors, the data was broken down by AOA into a training set and a test set to show generalization of the neural network to various AOA. Three neural network paradigms were used to model the data: 1) the multilayer perceptron (MLP)[7] trained with back propagation, 2) the radial basis function (RBF)[8] network trained with orthogonal least squares learning, and 3) the general regression neural network (GRNN).[9] The performance of each network on a 33-MHz, 386-based personal computer was recorded and the best results are tabulated in Table 1. Initially, the GRNN network appeared to be the most suitable choice for modeling the buffet data since it had the best training time and the least training error of the three networks. It also had a generalization capability as good as the RBF network and better than the MLP. Performance plots (Fig. 7) show that the GRNN had a greater ability to follow sharply changing trends in the data than either the RBF or the MLP.

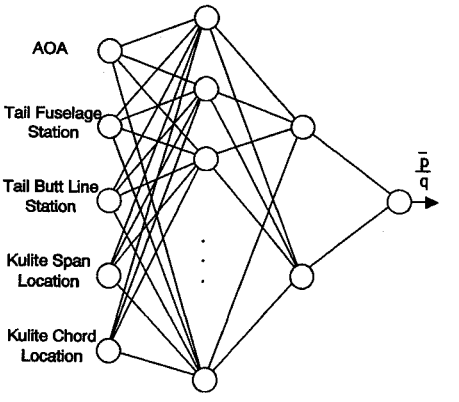

Fig. 6 Neural network for rms buffet load prediction.

After showing that all of the neural networks had the ability to generalize to new angles of attack, the next step was to show that reasonable pressures at any AOA could be predicted over the entire surface of the tail. Because both the GRNN and the RBF had significantly lower errors than the MLP, the MLP was eliminated at this stage of the evaluation.

Although the GRNN showed the most promise for AOA modeling, the statistical nature of the learning algorithm did not yield good results for prediction over the tail surface. When an input to the GRNN is far from the nearest density function, its best estimate must be based on the nearest joint density function. This property precludes extrapolation or even interpolation over long distances and is not desirable for buffet modeling.

Evaluation of the RBF network showed answers that would approach zero as testing inputs got further and further away from the nearest training input. The nature of the RBF network is that each node has a radius about which it will significantly activate. This property gives the RBF its fast learning capabilities because it only needs to change weights in a localized area. Extrapolation or distance interpolation becomes impossible for conventional RBF using Gaussian nodes because they will give a near-zero result away from their closest node. A solution to this problem was to replace the Gaussian activation function with a multiquadratic function. The advantage of the multiquadratic function is that it increases in a nonlinear manner instead of approaching zero. It is this characteristic that allows extrapolation to take place.

To verify that the RBF with the multiquadratic function could accomplish distance interpolation, and by extension extrapolation, the data measured from the center Kulite sensor was removed from the training set and the trained network was then tested to see how close it's estimation of the pressures in the center of the tail would come to the actual measurements. Figure 8 shows that the RBF network predicts the high AOA response very well, but underpredicts the response at low AOA. This indicates that additional sensor information would be required to accurately model this regime.

Having established the viability of the RBF network with the multiquadratic function, a pressure map of the entire tail was made. The RBF network was first trained using all available data, then rms pressures were generated at evenly spaced points along the surface of the tail (Fig. 9). Black represents the lower magnitudes of pressure, and white represents the highest pressures. The image presented is at 40-deg AOA,

Table 1 Comparison of neural network training methods

Output	Network name	Training time, s	Hidden nodes	Training rms error	Testing rms error
$\bar{p}/q$	MLP	12,452	15/5	0.009504	0.01901
	RBF	3,240	52	0.011664	0.01181
	GRNN	9	95	0.007200	0.01138
Bending moment	MLP	1,850	15	0.0034	0.0072
	RBF	27	24	0.0041	0.0041
	GRNN	<1	48	0.0004	0.0040
Torsion moment	MLP	1,850	15	0.0034	0.0072
	RBF	26	22	0.0050	0.0048
	GRNN	<1	48	0.0005	0.0047

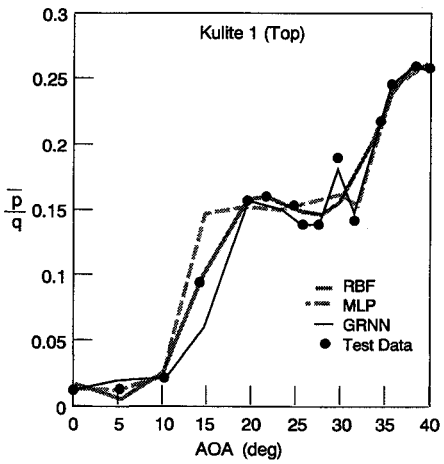

Fig. 7 $\bar{p}/q$ for inboard tail position for various networks (trained on half of data—225 points).

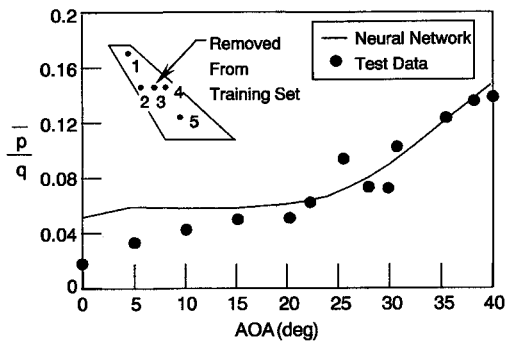

Fig. 8 RBF network with multiquadratic function (estimated pressures at Kulite no. 3).

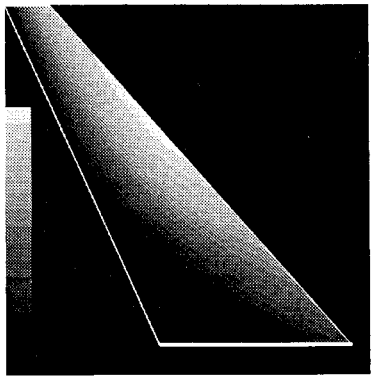

Fig. 9 Surface contours of rms pressure using neural network.

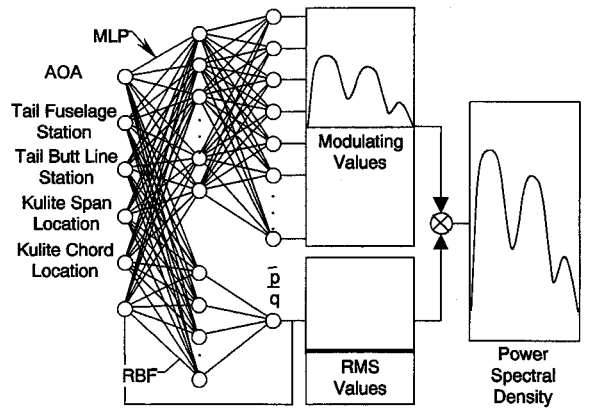

Fig. 10 RBF/MLP hybrid cascading neural network.

and the tail is located at the inboard tail position. Note that in general for any given AOA, the pressure increases toward the leading edge of the tail and decreases toward the trailing edge of the tail. While this image shows that the correct aerodynamic trends have been mapped, verification of these pressure distributions will come from correlation of flexible tail responses using finite element analysis.

Frequency Dependent Data Modeling

The next goal was to accurately predict the PSD of the buffet pressures. Data measurements were provided as in the section detailing rms pressures, with the addition of 49 nondimensional frequencies and their corresponding outputs (nondimensional pressure spectra values) for a total of 7350 input/output pairs.

The average magnitude of the buffet PSDs can vary from close to zero for low AOA, to curves that are 500 times as great for high AOA. Neural networks train by attempting to produce the lowest overall rms error. If, as in this case, some input vectors produce outputs that can be hundreds of times greater in magnitude than others, then the neural network will tend to concentrate its learning effort towards those outputs.

For these reasons, a scaling method had to be developed to equally emphasize both the lower and higher magnitude PSD curves within the network. The method that was developed combines the RBF network and a MLP network into a single hybrid cascading neural network (HCNN) (Fig. 10). The hybrid system works by using the RBF network developed in the first section of this article to predict the rms pressure level of the signal (curve). This pressure is fed back into the MLP along with the original inputs as shown, and these inputs are used to predict the modulating signal. The MLP shown has 49 outputs that correspond to the 49 frequencies of the training data. This signal has approximately the same magnitude for any input, thus focusing the MLP on the shape of the modulating signals instead of their relative

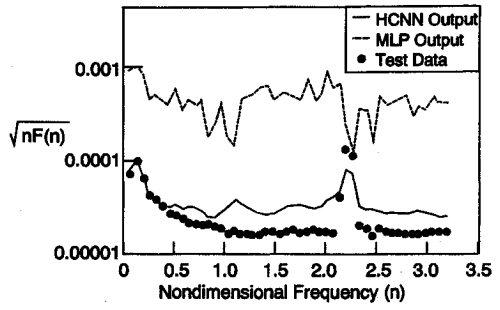

Fig. 11 Comparison of network architecture's effect on prediction of pressure spectra.

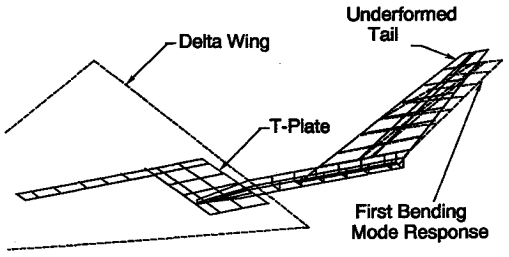

Fig. 12 NASTRAN finite element model of flexible tail and support structure.

magnitudes. The entire process is performing a dynamic scaling where the rms pressure generated from the RBF is used to scale (and later unscale) the PSD. Finally, the rms signal and the modulating signal are passed through a multiplier to reconstruct the final unscaled PSD curve. The effectiveness of this approach on maintaining signal shape can be seen by comparing the best results of a single neural network (MLP) and the results of the hybrid cascading neural network (Fig. 11). Note the HCNN effectively removes the problem of magnified noise. The hybrid cascading neural network is able to maintain the same amount of overall error in the testing set as the single neural network. Its ability to maintain the correct shape and identify modes in the PSD make its increased complexity worthwhile. Overall rms error magnitude in the final solution was approximately 5% for the entire range of PSD values. With the established neural network prediction for PSDs, the final finite element correlations could be made.

Finite Element Modeling

An elastic finite element model was used to take the rigid tail PSD pressure distributions predicted by HCNN and use them to predict the bending moments at the base of the flexible vertical tail and verify experimental results. The neural network was trained on the pressures from the five sensor positions on the vertical tail and is able to extrapolate pressures over the entire area of the tail to supply refined pressure distributions to the finite element model. It should be noted that the neural network provides an unbiased method of distributing pressures measured at only five points on the tail over the entire surface of the tail. However, the network is not creating new data, and therefore, is only as robust as the original measurands. Three parts of the wind-tunnel model were modeled using NASTRAN and are shown in Fig. 12. The T-plate is a 0.3-in.-thick piece of steel that bolts onto the rear of the delta wing and provides attachment points for the vertical tail. The T-plate is symmetric about the wing centerline, and so half of the plate was modeled with plate elements. The DOF on the T-plate model at the wing attachment locations were constrained. An aluminum boom attaches with screws to the T-plate in one of three positions that correspond to the three lateral tail positions tested in the wind tunnel.[1] The boom is a rod with one end machined flat that attaches to the T-plate and a channel machined into the remainder of its length for the vertical tail to sit in. The boom was modeled

Table 2 Comparison of ground vibration test frequencies

Mode of vertical tail	NASA LaRC tests, Hz	MDA tests, Hz	MDA FEM,[a] Hz
1st Bending	33	31	31
2nd Bending	180	168	153
1st Torsion	307	280	292
3rd Bending	430	406	417

[a]Finite element modeling.

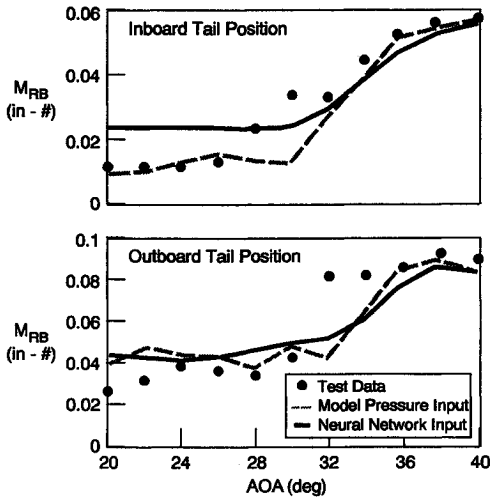

Fig. 13 Comparison of analytical and experimental flexible response.

with plate elements and solid elements. The vertical tail is 4 in. tall with a 53.5-deg sweep angle. It attaches to the boom with four bolts at three locations corresponding to the three fore-aft positions tested. The single aluminum spar and balsa wood covering that make up the flexible vertical tail were both modeled with plate elements. In the NASTRAN model the T-plate, boom, and vertical tail were connected together in the desired configuration by using rigid bars to connect the appropriate grid points together.

Ground vibration tests (GVT) were performed to find the natural frequencies and corresponding mode shapes of the structure. A GVT was performed by NASA LaRC on the T-plate, boom, and flexible vertical tail. MDA performed a GVT on the flexible vertical tail and obtained results comparable to those obtained at Langley as shown in Table 2. Each of the three finite element models were refined to agree with the GVT results by using a series of spring elements at the root of the tail to account for inherent attachment flexibility.

Two sets of random forced response solutions were run on the correlated NASTRAN model. The first set consisted of a segmented grid of pressures which were simply given a PSD value from one of the five Kulites based on a best-guess distribution of the test data. The second set used unique PSD information for each grid based on the neural network prediction. In both cases the same cross spectral densities were included directly from the test data since the neural network was not trained on this information. NASTRAN was also used to include the effects of aerodynamic damping on the response. Solutions were run for AOAs from 20 to 40 deg, and the results are shown for the outboard and inboard tail positions (Fig. 13). For the outboard tail position, both the model pressure and neural network loading inputs matched test results within 10% in the 32–40-deg AOA range. Between 28–32 deg the neural network loads yield a significant improvement over the best-guess distribution. Below 26 deg the neural network overpredicts the tail response. Due to the minimal number of Kulites and the limitations of the multiquadratic function in the neural network, this result at low excitation levels is not unusual and will be addressed in future work. The inboard tail position, which had much higher buffet

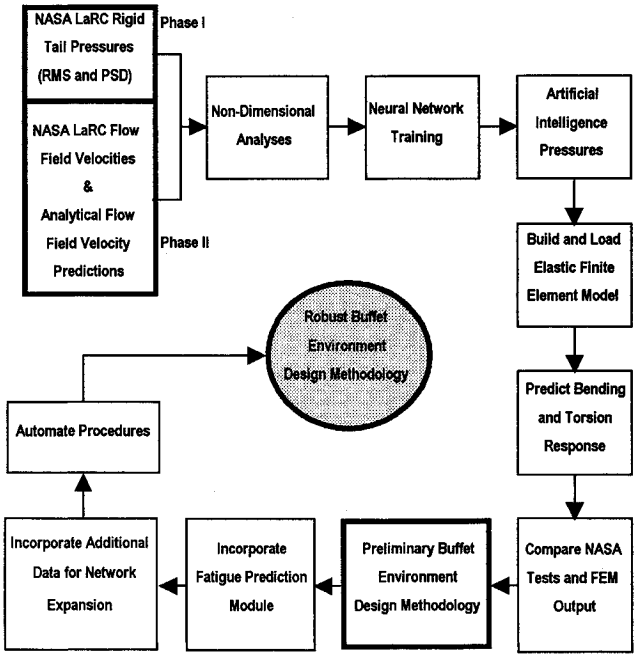

Fig. 14 MDA/NASA vortex-tail interaction research objectives.

response, shows a much improved overall correlation of neural network loading and the test data. Neither the direct test input pressures nor the neural network predicted the 32-deg response closely. This effect is most likely due to the minimal amount of Kulite pressure information from which to base the dynamics loads upon. In general, the neural network pressure load predictions provide a reasonable estimate of elastic response when applied to the NASTRAN model. This result verifies that the method of using neural networks trained with experimental buffet data can be utilized for advanced design of empennage structures where similar vortex phenomena may exist.

Empennage Design Using Neural Networks

Based on the neural network/finite element methods discussed above, artificial neural network systems can be developed to incorporate more detailed upstream information in order to divorce geometric influences from flowfield parameters. In the near future, upstream velocity measurements will be acquired with an LDV as part of the NASA/MDA vortex-tail interaction investigation. These velocity measurements will be reduced and incorporated into the HCNN. Once this link has been established for one planform-empennage type of configuration, others can be added to the self-learning neural network system to yield a more robust artificial intelligence system for various aircraft configurations (Fig. 14). This can be done through the use of existing test data from present day aircraft or additional wind-tunnel tests. The objective of the artificial neural network buffet prediction system is to be able to determine fluctuating pressure loads on new aircraft configurations. To achieve this goal, CFD or analytical flowfield velocity contour characteristics upstream of a vortex burst point can be used in lieu of actual test data as inputs to the trained neural network to predict empennage response. These advanced design pressure predictions can then be applied to a finite element model to predict elastic structural response as discussed within. This design approach provides a means to fold in complicated vortex physical phenomena into an artificial neural network system that in turn can be used effectively and quickly in advanced design for detailed tail sizing, location, and structural design.[10]

Concluding Remarks

The cooperative NASA/MDA vortex-tail interaction research program has provided the data base of information for the development of an artificial neural network empennage load prediction system. Neural networks have been shown to be a viable way to model vortex-tail interaction buffet data. They have the ability to use many input combinations to produce an accurate output and have shown themselves able to generalize well for differing AOA. Flexible response from the elastic model have validated the accuracy of the neural network predicted pressures when compared with test data. During this investigation it was found that spatial correlation of pressure PSDs is very important in obtaining good flexible response results. Future tests with a more detailed pressure sensor layout should provide the necessary information to predict optimum grid size application for neural network pressure values.

This program has been the first step towards a methodology that incorporates experimental data, neural networks, finite element modeling, and nondimensionalization techniques into an integrated buffet design approach.

References

[1]Washburn, A. E., Jenkins, L. N., and Ferman, M. A., "Experimental Investigation of Vortex-Fin Interaction," AIAA Paper 93-0050, Jan. 1993.

[2]Zimmerman, N. H., Ferman, M. A., and Yurkovich, R. N., "Prediction of Tail Buffet Loads for Design Applications," AIAA Paper 89-1378, April 1989.

[3]Ferman, M. A., Patel, S. R., Zimmerman, N. H., and Gerstenkorn, G., "A Unified Approach to Buffet Response," 70th Meeting of Structures and Materials Panel, AGARD 17, Sorento, Italy, April 1990.

[4]Mabey, D. G., "Some Aspects of Aircraft Dynamic Loads due to Flow Separation," AGARD Rept. 750, 1988.

[5]Roos, F., and Kegelman, J. T., "Recent Explorations of Leading Edge Vortex Flowfields," High Angle of Attack Technology Conf., NASA Langley, Oct.–Nov., 1990.

[6]Lippmann, R. P., "An Introduction to Neural Computing with Neural Nets," *IEEE ASSP Magazine*, April 1987, pp. 4–22.

[7]Rumelhart, D. E., and McClelland, J. L., "Parallel Distributed Processing," *Foundations*, Vol. 1, PDP Research Group, MIT Press, Cambridge, MA, 1986, Chap. 8.

[8]Chen, S., Cowan, C. F. N., and Grant, P. M., "Orthogonal Least Squares Learning Algorithm for Radial Basis Function Networks," *IEEE Transactions on Neural Networks*, Vol. 2, No. 2, 1991, pp. 302–309.

[9]Specht, D. F., "A General Regression Neural Network," *IEEE Transactions on Neural Networks*, Vol. 2, No. 6, 1991, pp. 568–576.

[10]McDonnell Douglas Aerospace, "Dynamic Loads and Response," Independent Research and Development, PD no. 7-360, Q0804-7, Feb. 1992.